Supporting Information

Characterization of a K^+-Induced Conformational Switch in a Human Telomeric DNA Oligonucleotide Using 2-Aminopurine Fluorescence

Robert D. Gray[†], Luigi Petraccone[†,§], John O. Trent[†] and Jonathan B. Chaires[†,]*

[†]James Graham Brown Cancer Center, University of Louisville, Louisville, KY 40202 and [§]Department of Chemistry "P. Corradini", University of Naples Federico II, 80126 Naples, Italy

Figure S1. Spectrophotometric titrations of 2-AP derivatives of Tel22 with KCl or NaCl. Titrations were carried out in 10 mM tetrabutyl ammonium phosphate buffer (Bu_4AmP), 1 mM EDTA, pH 7.0 at 25 ºC as described in reference (*1*). The spectra in the panels on the left are presented as difference spectra where ε_U is the absorptivity of the unfolded state and ε_F is the absorptivity of the folded state. The panels on the right show *Y*, the fractional change in the change in absorbance at 295 nm *vs*. log [salt]. The lines represent the best fit of the points to the Hill equation $Y = Y_{max} \cdot [M^+]^n / \{(K_{0.5})^n + [M^+]^n\}$ estimated by non-linear least squares as described in reference (*1*). The errors are standard deviations of the fitted parameters.

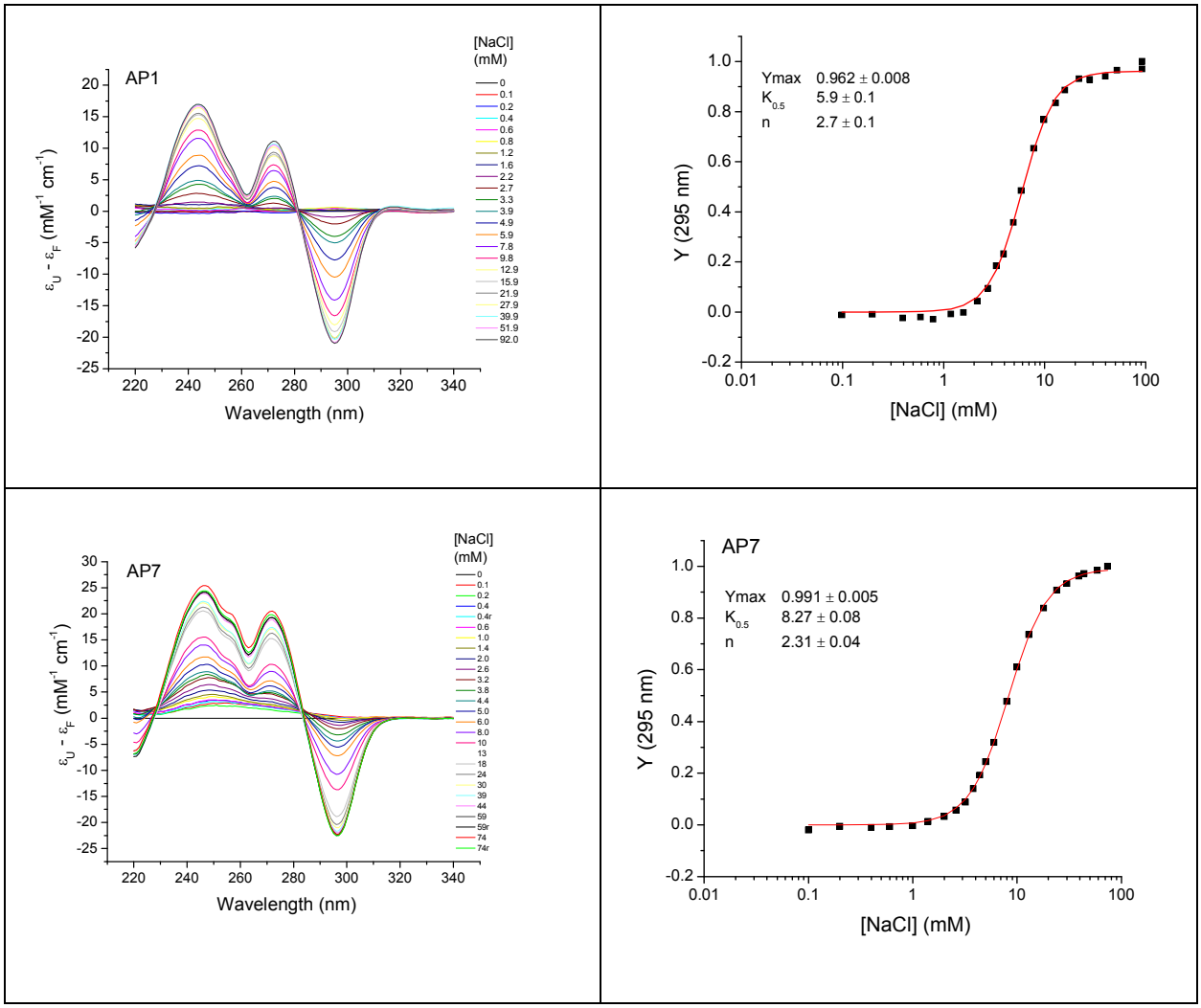

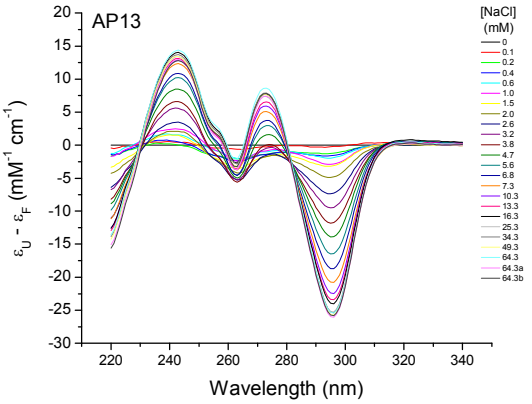
AP13
[NaCl] (mM)
0
0.1
0.2
0.4
0.6
1.0
1.5
2.0
2.6
3.2
3.8
4.7
5.6
6.8
7.3
10.3
13.3
16.3
25.3
34.3
49.3
64.3
64.3a
64.3b
$\varepsilon_U - \varepsilon_F$ (mM^{-1} cm^{-1})
Wavelength (nm)

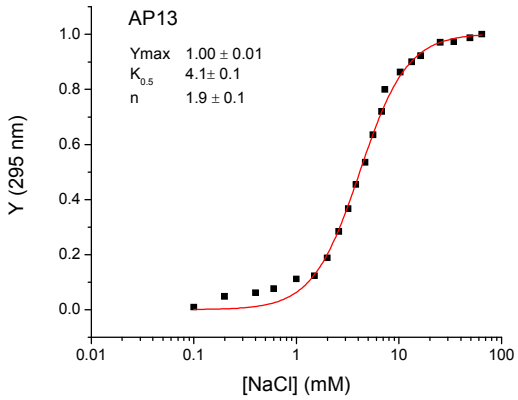
AP13
Ymax 1.00 ± 0.01
$K_{0.5}$ 4.1± 0.1
n 1.9 ± 0.1
Y (295 nm)
[NaCl] (mM)

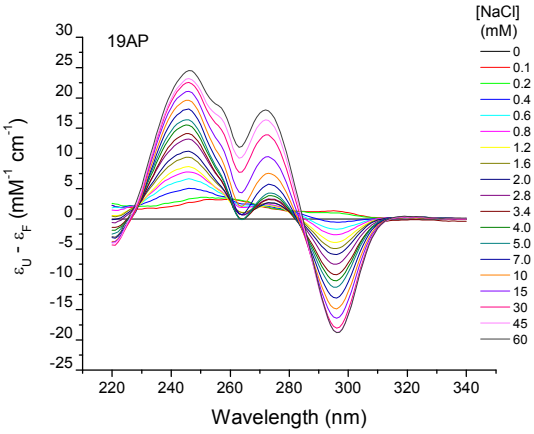
19AP
[NaCl] (mM)
0
0.1
0.2
0.4
0.6
0.8
1.2
1.6
2.0
2.8
3.4
4.0
5.0
7.0
10
15
30
45
60
$\varepsilon_U - \varepsilon_F$ (mM^{-1} cm^{-1})
Wavelength (nm)

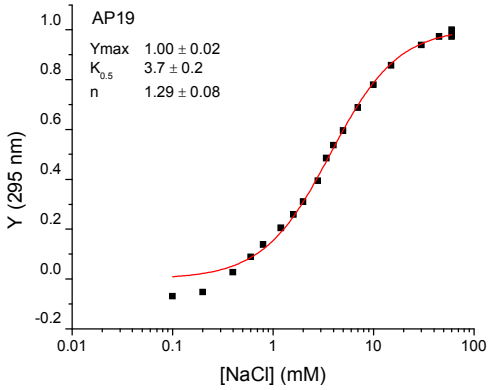
AP19
Ymax 1.00 ± 0.02
$K_{0.5}$ 3.7 ± 0.2
n 1.29 ± 0.08
Y (295 nm)
[NaCl] (mM)

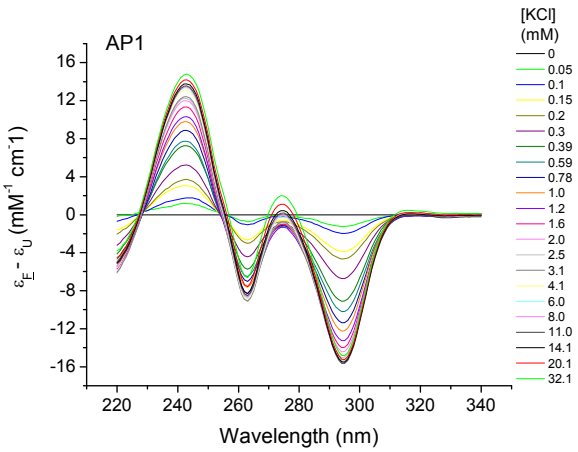
AP1
[KCl] (mM)
0
0.05
0.1
0.15
0.2
0.3
0.39
0.59
0.78
1.0
1.2
1.6
2.0
2.5
3.1
4.1
6.0
8.0
11.0
14.1
20.1
32.1
$\varepsilon_F - \varepsilon_U$ (mM^{-1} cm^{-1})
Wavelength (nm)

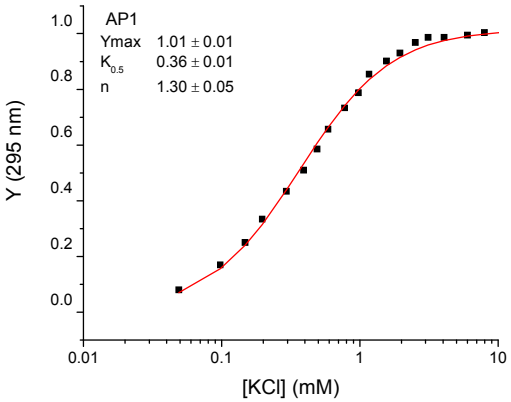
AP1
Ymax 1.01 ± 0.01
$K_{0.5}$ 0.36 ± 0.01
n 1.30 ± 0.05
Y (295 nm)
[KCl] (mM)

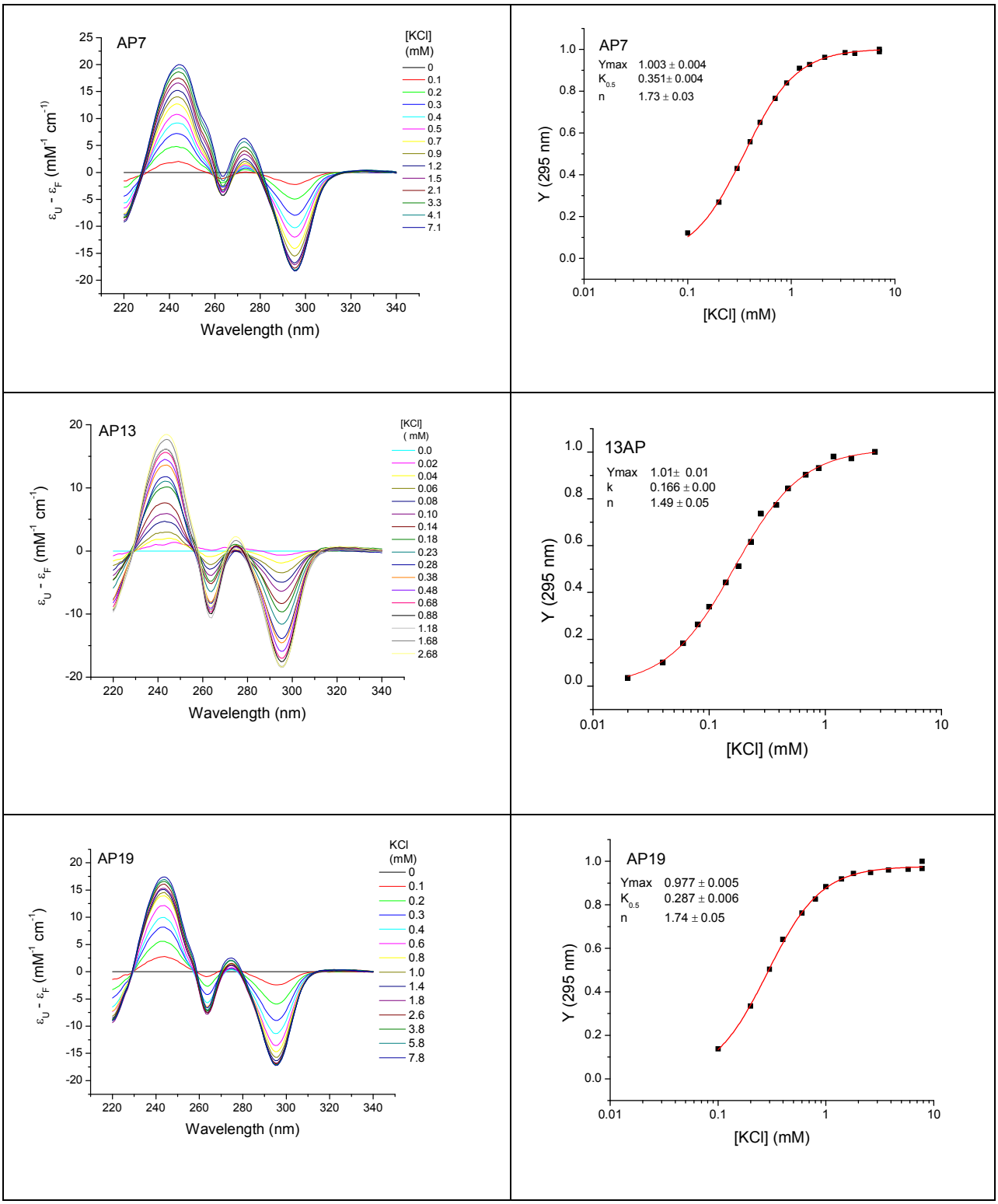
AP7
[KCl] (mM)
0
0.1
0.2
0.3
0.4
0.5
0.7
0.9
1.2
1.5
2.1
3.3
4.1
7.1
$\varepsilon_U - \varepsilon_F$ (mM^{-1} cm^{-1})
Wavelength (nm)
AP7
Ymax 1.003 ± 0.004
$K_{0.5}$ 0.351± 0.004
n 1.73 ± 0.03
Y (295 nm)
[KCl] (mM)
AP13
[KCl] (mM)
0.0
0.02
0.04
0.06
0.08
0.10
0.14
0.18
0.23
0.28
0.38
0.48
0.68
0.88
1.18
1.68
2.68
$\varepsilon_U - \varepsilon_F$ (mM^{-1} cm^{-1})
Wavelength (nm)
13AP
Ymax 1.01± 0.01
k 0.166 ± 0.00
n 1.49 ± 0.05
Y (295 nm)
[KCl] (mM)
AP19
KCl (mM)
0
0.1
0.2
0.3
0.4
0.6
0.8
1.0
1.4
1.8
2.6
3.8
5.8
7.8
$\varepsilon_U - \varepsilon_F$ (mM^{-1} cm^{-1})
Wavelength (nm)
AP19
Ymax 0.977 ± 0.005
$K_{0.5}$ 0.287 ± 0.006
n 1.74 ± 0.05
Y (295 nm)
[KCl] (mM)

Figure S2. Titration of Tel22 with NaCl determined by CD. Panel A shows the CD spectra of Tel22 at various NaCl concentrations. The vertical arrows indicate the direction of the changes in ellipticity with increasing [cation]. The NaCl concentrations are in Table S1. Panel B shows the values of the ellipticity at 295 nm as a function of [NaCl]. The lines show the least squares fit of the data points to eq. 3 in the text. The optimal fitting parameters for these curves are given in Table 1 of the text. Panel C shows the calculated CD spectra of the unfolded and unfolded states and Panel D shows the [NaCl]-dependence of the two significant spectroscopic species throughout the titration. The CD spectra of the significant spectroscopic species and their concentration profiles were calculated from the spectral titration data in Panel A by SVD analysis coupled with the model-free evolving factor analytical procedure as described in the text. The detailed results of the SVD analysis are given in Figure S3. Conditions: [Tel22] = 6.7 μM in 10 mM Bu_4AmP, 1 mM EDTA, pH 7.00. Temperature = 25 ºC.

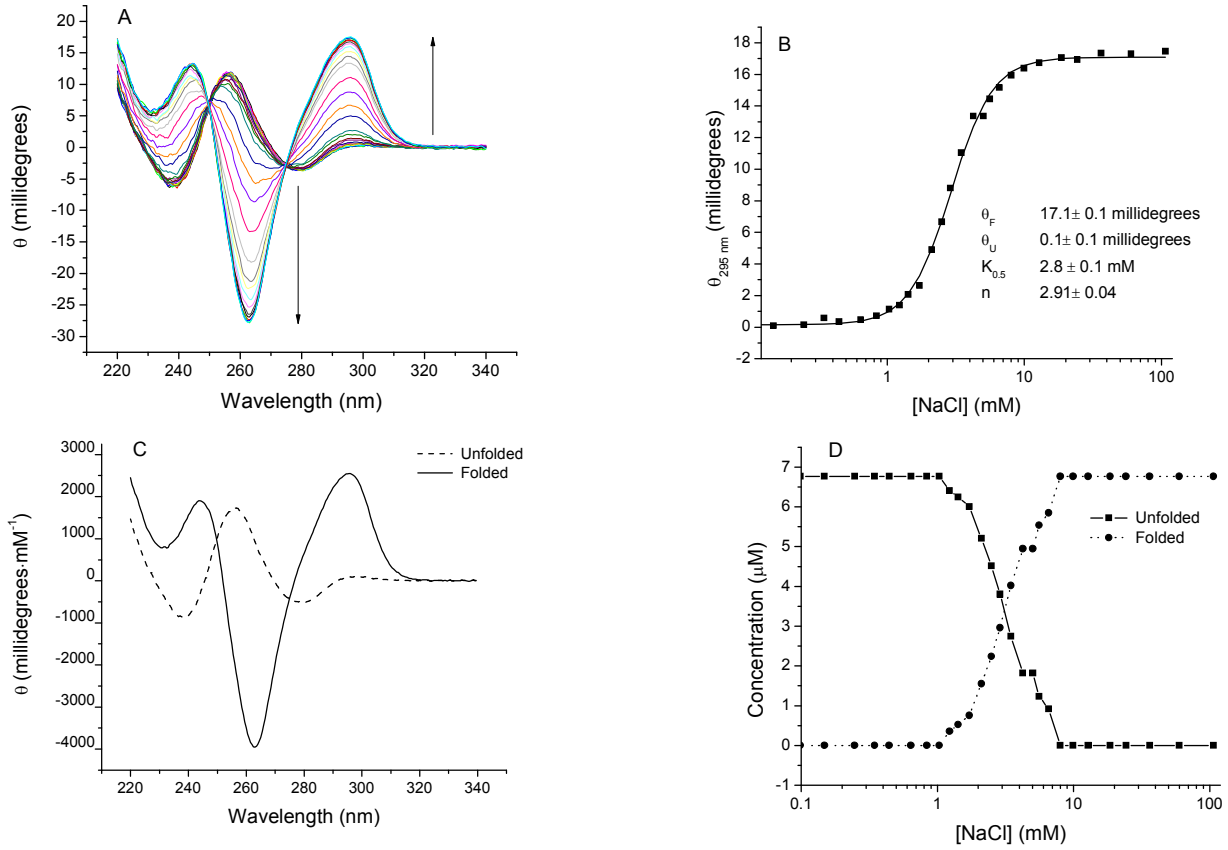

Figure S3. SVD analysis of CD titration of Tel22 with NaCl. Panel A shows the first four basis spectra and Panel B shows the magnitude of the corresponding amplitude vectors for the experimental data shown in Figure 4A. Panel C shows the first 10 singular values derived from the SVD analysis and panel D shows the autocorrelation coefficients for the first 10 elements of the U and V matrices. An autocorrelation coefficient >0.7 suggests that two spectral species, the unfolded and fully folded entities, contribute the KCl-induced changes in ellipticity.

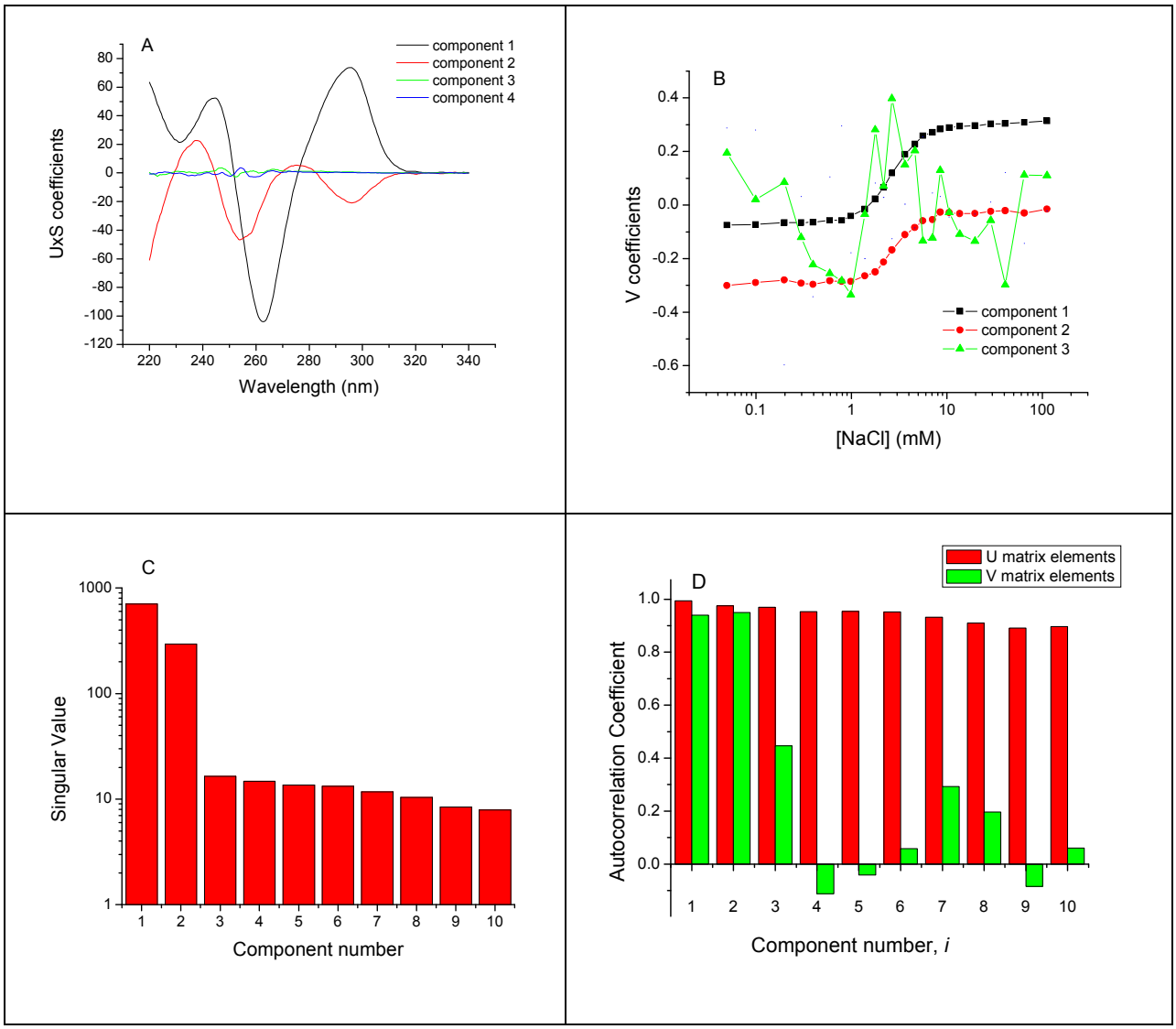

Figure S4. SVD analysis of CD titration of Tel22 with KCl. Panel A shows the first four basis spectra and Panel B shows the magnitude of the corresponding amplitude vectors for the experimental data shown in Figure 4E. Panel C shows the first 10 singular values derived from the SVD analysis and panel D shows the autocorrelation coefficients for the first 10 elements of the U and V matrices. An autocorrelation coefficient >0.7 suggest that three spectral species, the unfolded ensemble, an intermediate species and the fully folded species contribute the KCl-induced changes in ellipticity.

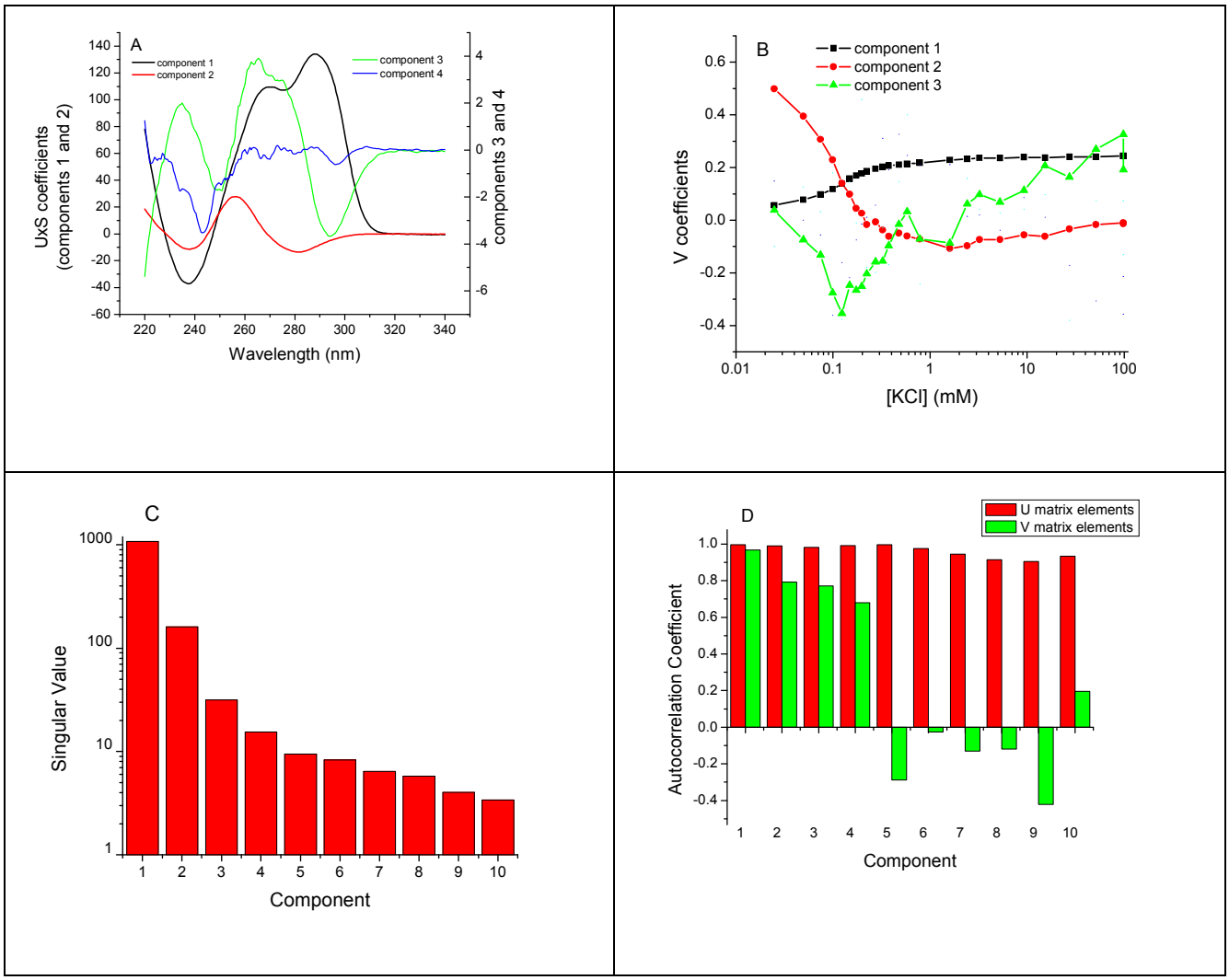

Figure S5. Stopped-flow kinetic analysis of the NaCl-induced folding of the 2-AP derivatives of Tel22. The panels on the right show the progress curves for NaCl-induced folding of 2-AP derivatives of Tel22 determined by rapid scanning multi-wavelength stopped-flow spectrophotometry. The kinetic data were fit to a sum of three exponentials using the program SpecFit/32 as described in reference *(1)*. In the panels on the right, the data points in black show the absorbance changes determined at 295 nm and the red line shows the globally determined best fit to the data points using the rate constants shown in the figure. The blue points show the residuals of the fit. The panels on the left show the calculated difference spectra $\Delta\varepsilon = \varepsilon_U - \varepsilon_F$ for the spectroscopically significant species for a triple exponential mechanism: U $\rightarrow$ I1 $\rightarrow$ I2 $\rightarrow$ F. Conditions: [Tel22] = 5-8 μM and [NaCl] = 100 mM (after mixing) in 10 mM Bu_4AmP, 1 mM EDTA, pH 7.0, 25 ºC. Cuvette pathlength = 2 cm.

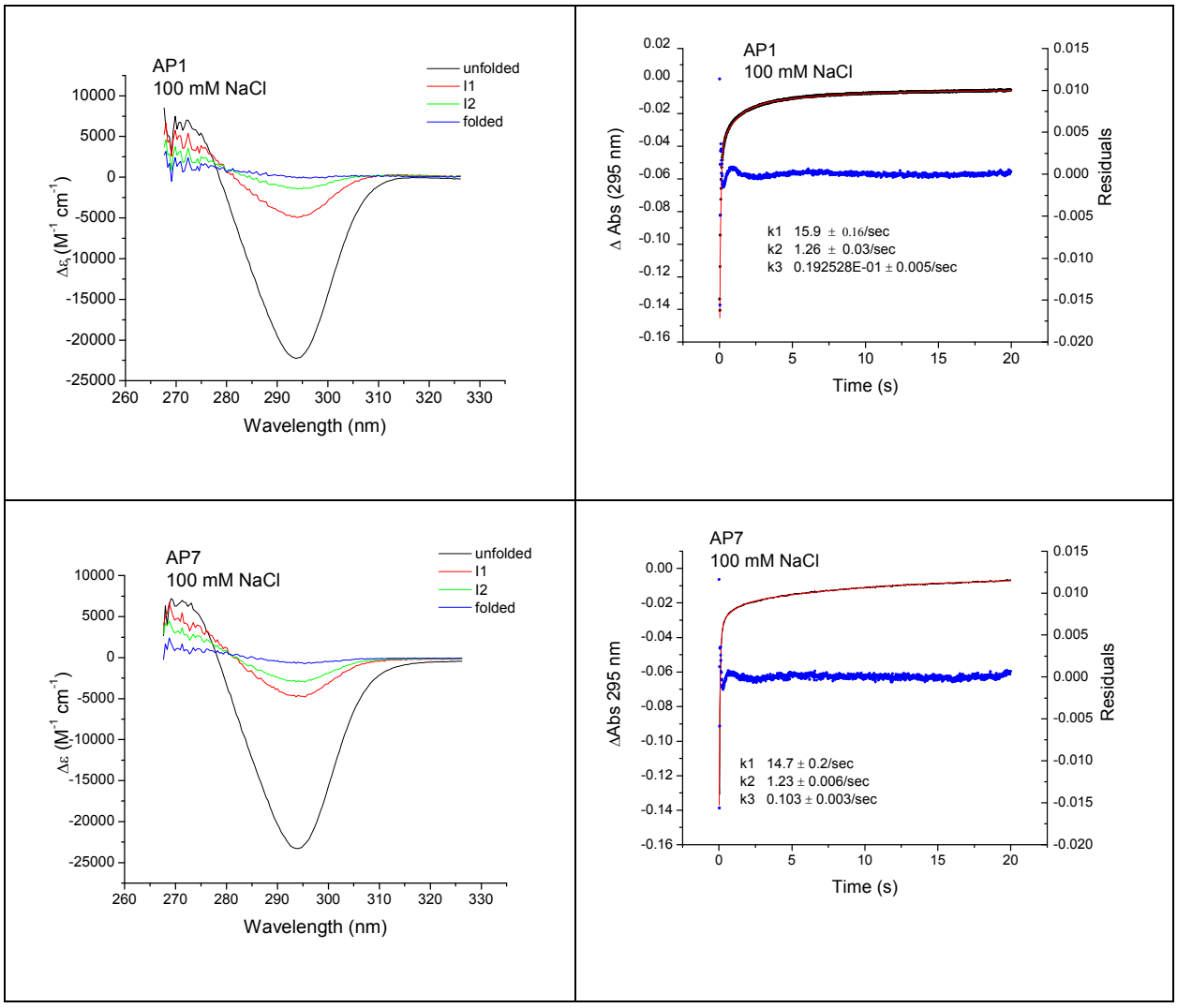

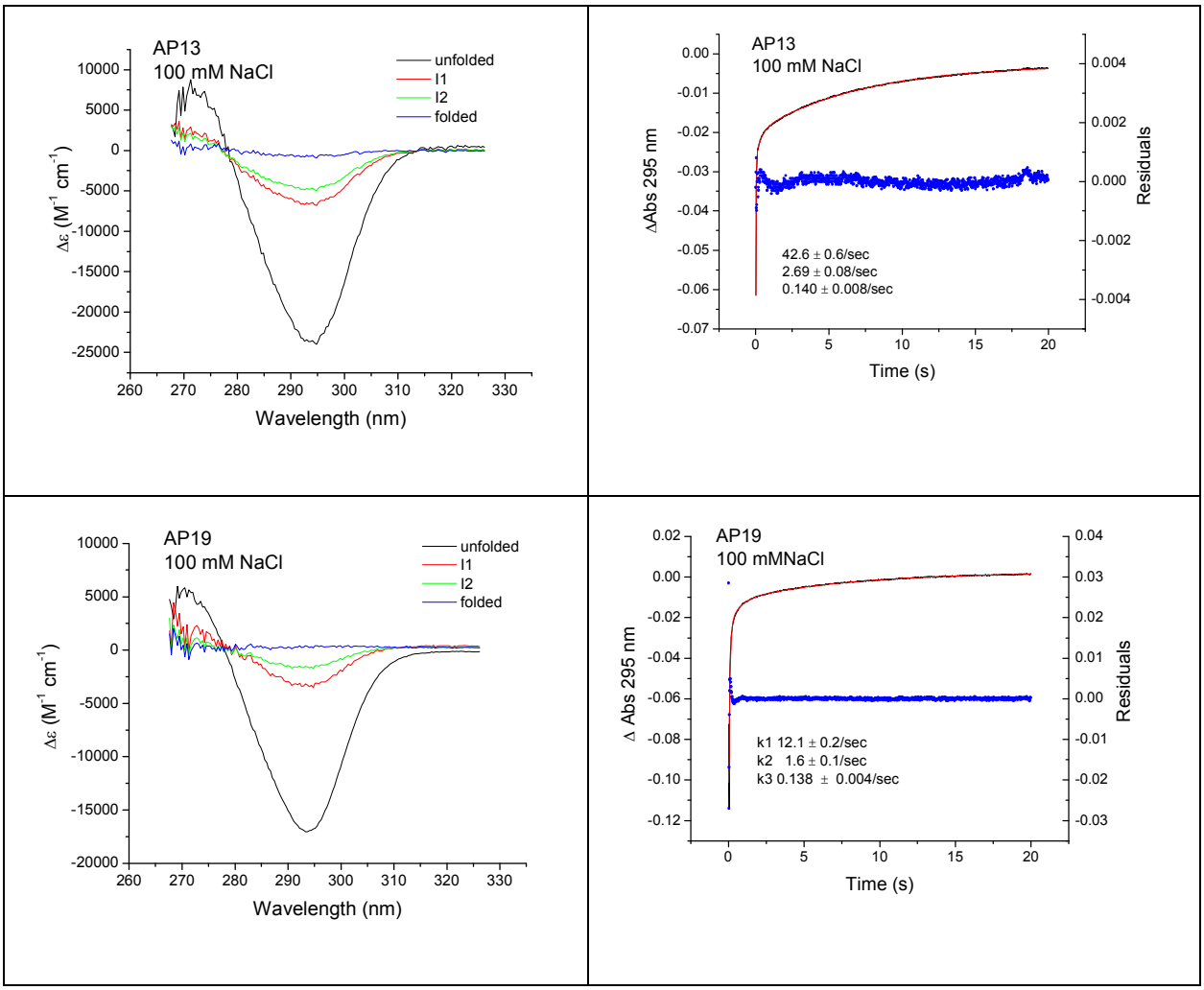
AP13
100 mM NaCl
unfolded
I1
I2
folded
Δε (M-1 cm-1)
Wavelength (nm)
AP13
100 mM NaCl
ΔAbs 295 nm
Residuals
42.6 ± 0.6/sec
2.69 ± 0.08/sec
0.140 ± 0.008/sec
Time (s)
AP19
100 mM NaCl
unfolded
I1
I2
folded
Δε (M-1 cm-1)
Wavelength (nm)
AP19
100 mMNaCl
Δ Abs 295 nm
Residuals
k1 12.1 ± 0.2/sec
k2 1.6 ± 0.1/sec
k3 0.138 ± 0.004/sec
Time (s)

Figure S6. Kinetics of changes in 2-AP fluorescence accompanying Na^+-induced folding of Tel22-2-AP derivatives. The data in the panels on the left were obtained by stopped-flow mixing. The data in the panels on the right were obtained by manual mixing. The grey points show the fluorescence intensity at 370 nm in counts/sec (cps) immediately prior to addition of NaCl. The black points show the changes in fluorescence after NaCl addition. In all cases, there was an "instantaneous" change in emission that occurred during the mixing period. The red line shows the best fit of the data to a single relaxation using the optimized parameters shown in each panel. *y0* is the equilibrium value of the fluorescence intensity, *A1* is a pre-exponential factor and *τ1* is the relaxation time. The errors given represent the standard deviation of the fitted parameters. The data points in grey which represent were not included in the fitting process.

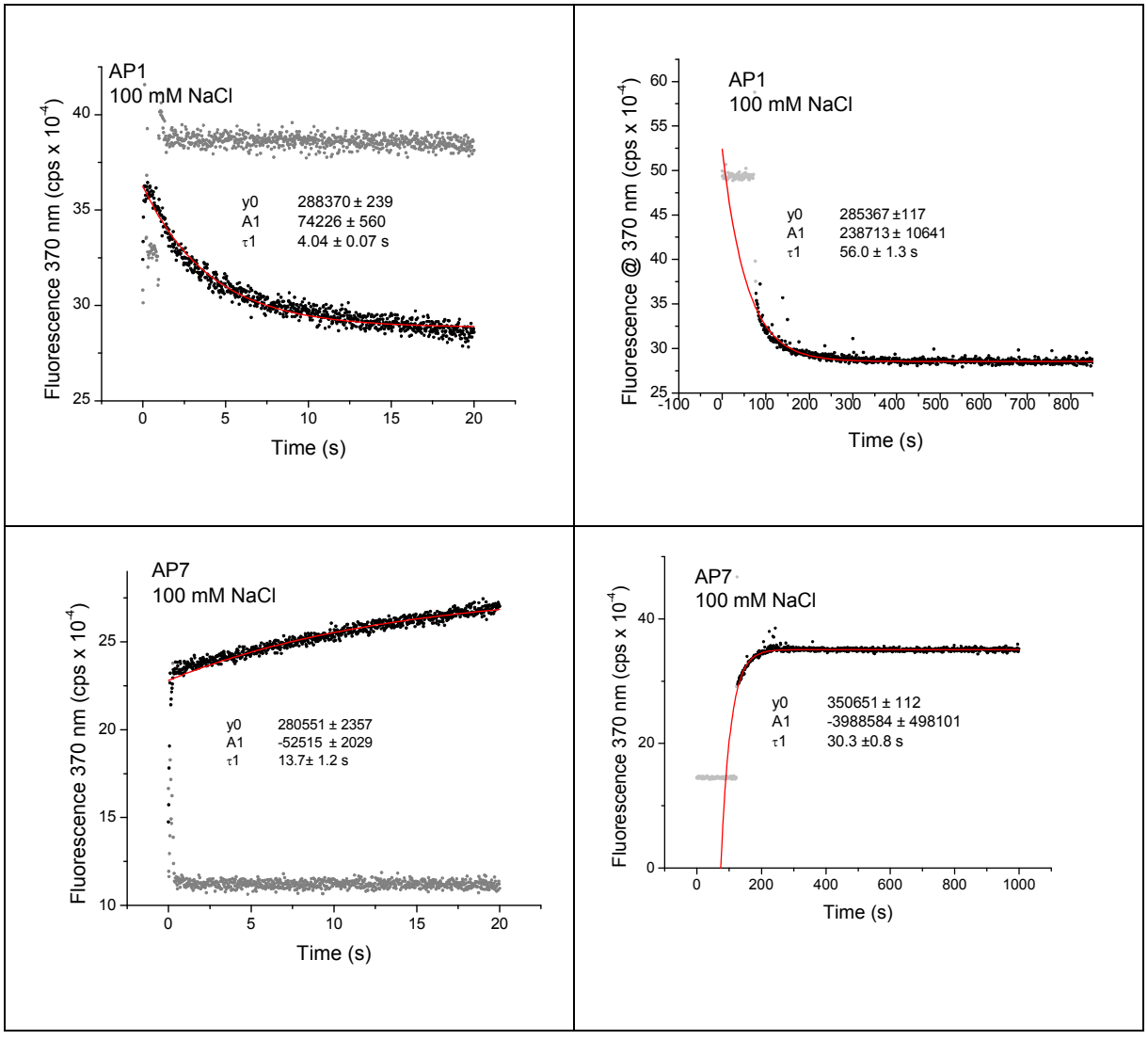

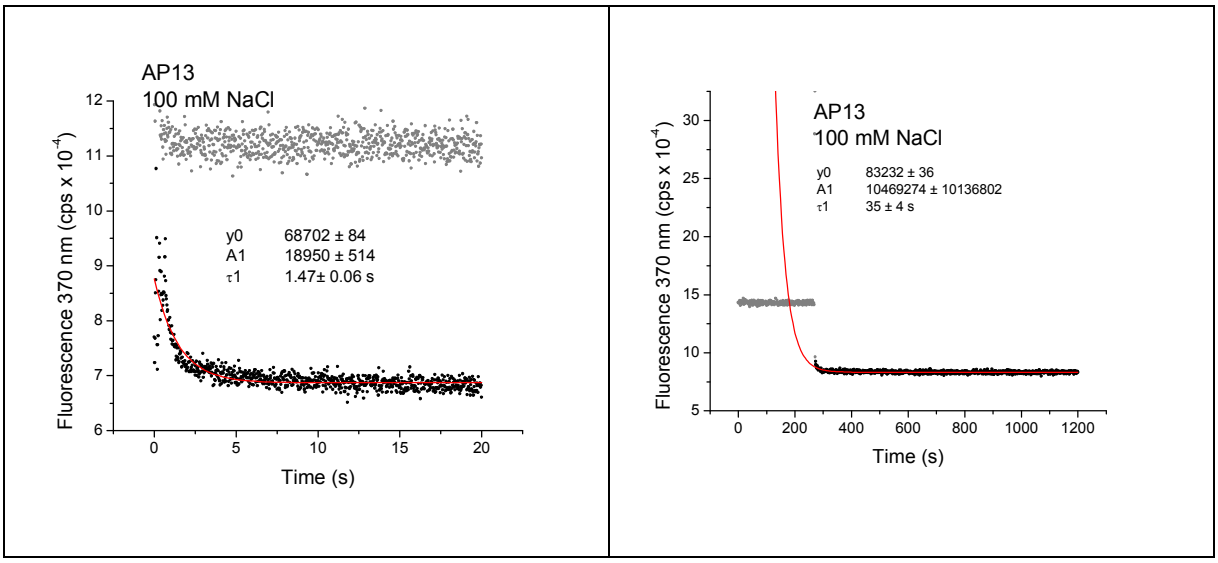
AP13
100 mM NaCl
y0 68702 ± 84
A1 18950 ± 514
τ1 1.47± 0.06 s
Fluorescence 370 nm (cps x 10^-4)
Time (s)
AP13
100 mM NaCl
y0 83232 ± 36
A1 10469274 ± 10136802
τ1 35 ± 4 s
Fluorescence 370 nm (cps x 10^-4)
Time (s)

Figure S7. Stopped-flow kinetic analysis of the KCl-induced folding of the 2-AP derivatives of Tel22. The panels on the right show the progress curves for KCl-induced folding of 2-AP derivatives of Tel22 determined by rapid scanning multi-wavelength stopped-flow spectrophotometry. The kinetic data were fit to a single exponential using the program SpecFit/32 as described in reference *(1)*. In the panels on the right, the data points in black show the experimentally determined absorbance changes at 295 nm and the red line shows the globally determined best fit to the data points using the rate constants shown in the figure. The blue data points show the residuals of the fit. The panels on the left show the calculated difference spectra $\Delta\varepsilon = \varepsilon_U - \varepsilon_F$ for the spectroscopically significant species for a single step mechanism: U $\rightarrow$ F. Conditions: [Tel22] = 5-8 μM and [KCl] = 50 mM (after mixing) in 10 mM Bu_4AmP, 1 mM EDTA, pH 7.0, 25 ºC. Cuvette pathlength = 2 cm.

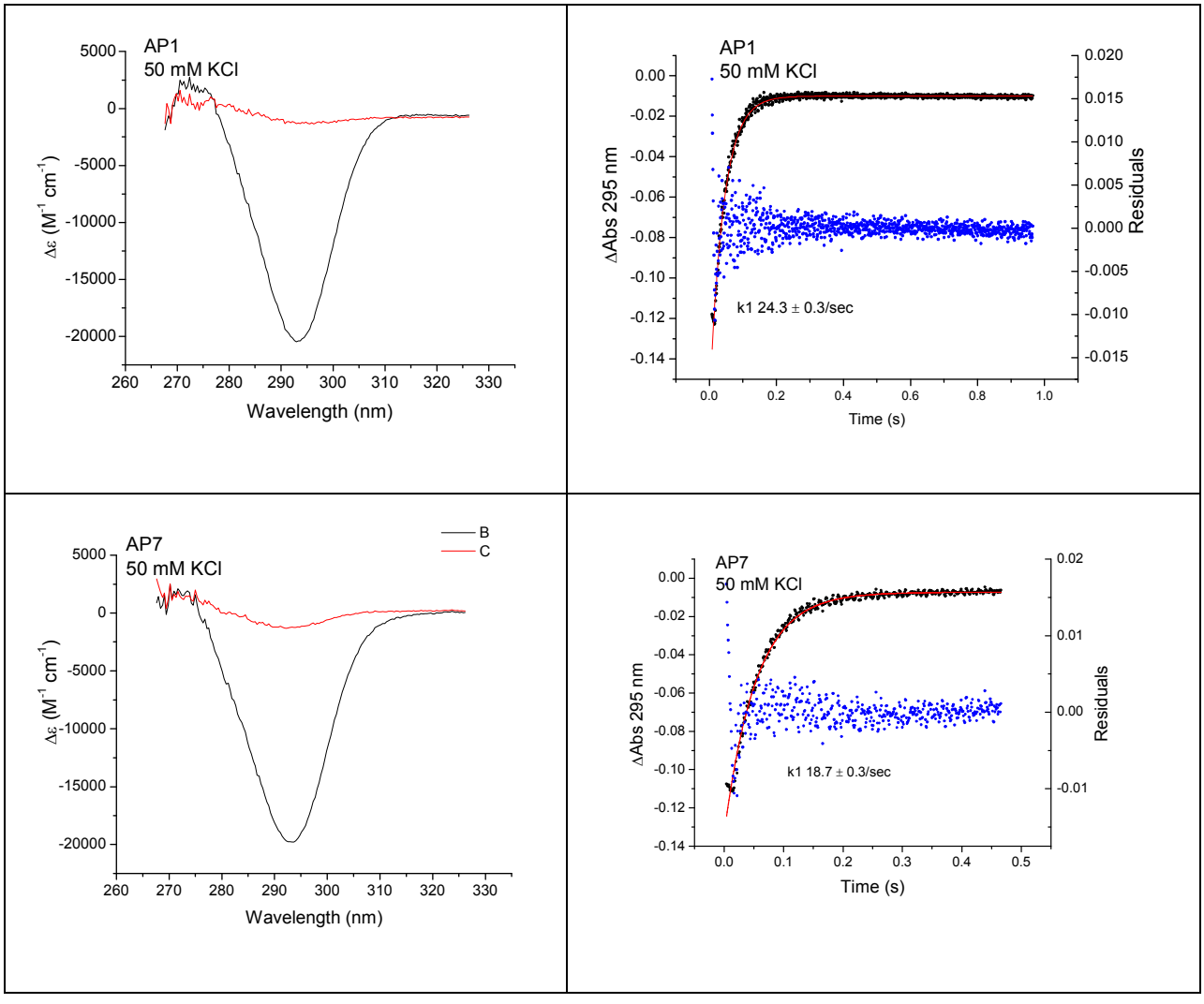

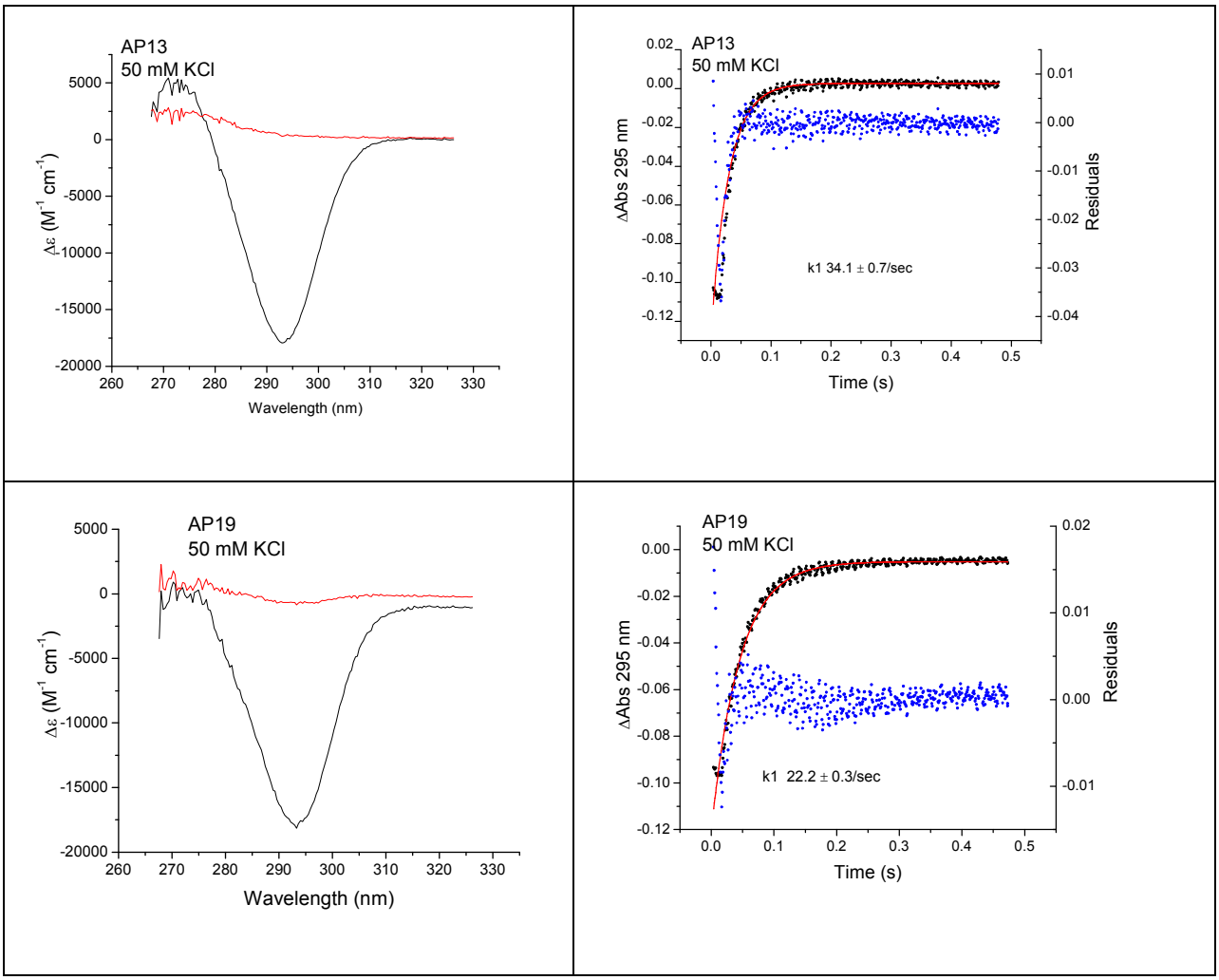
AP13
50 mM KCl
Δε (M-1 cm-1)
Wavelength (nm)
AP13
50 mM KCl
ΔAbs 295 nm
Residuals
k1 34.1 ± 0.7/sec
Time (s)
AP19
50 mM KCl
Δε (M-1 cm-1)
Wavelength (nm)
AP19
50 mM KCl
ΔAbs 295 nm
Residuals
k1 22.2 ± 0.3/sec
Time (s)

Figure S8. Kinetics of changes in 2-AP fluorescence accompanying K^+-induced folding of Tel22 derivatives. Panels A-D show progress curves obtained by stopped-flow mixing of 2AP-Tel22 oligonucleotides with [KCl] (50 mM). The grey data points show the fluorescence intensity immediately prior to mixing, the black points show fluorescence after KCl addition and the red lines show the fit of the data to one or two relaxations by non-linear least squares using the optimized parameters given in figures. *y0* is the final equilibrium value of the fluorescence, A_i is the pre-exponential factor and τ_i is the corresponding relaxation time. The errors are the standard deviation of the fitted parameters.

Panels A-D:

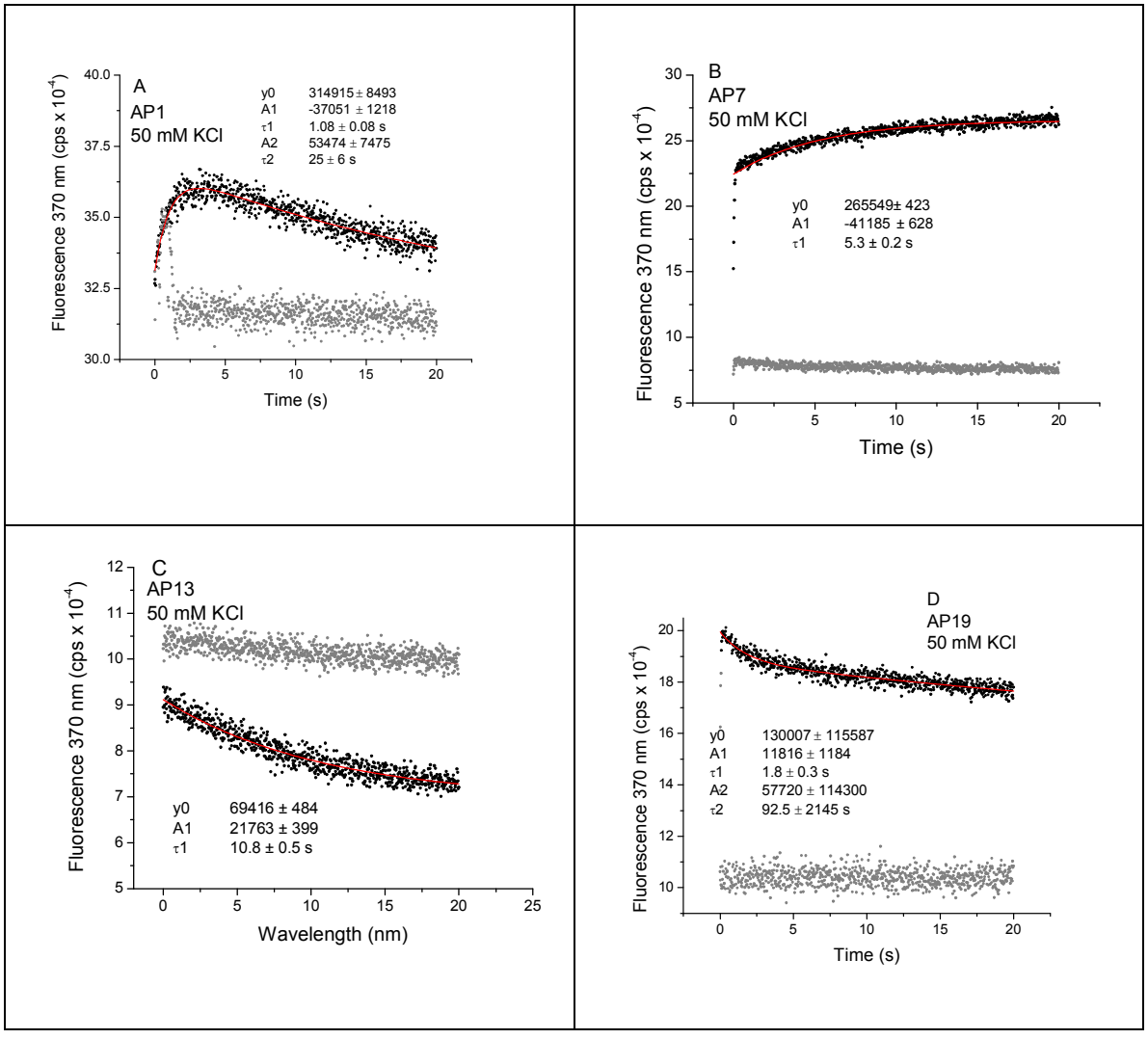

Panels E-J: Kinetics of fluorescence changes following manual mixing of the indicated oligonucleotide to give 3 mM KCl (left panels) or 50 mM KCl (right panels). The data points in grey are represent the fluorescence prior to adding KCl. The black points are the experimental data and the red line represents the best fit of the data represented by the black points to one or two relaxations. *y0* is the final equilibrium value of the fluorescence, A_i is the pre-exponential factor and τ_i is the corresponding relaxation time. The errors are the standard deviation of the fitted parameters.

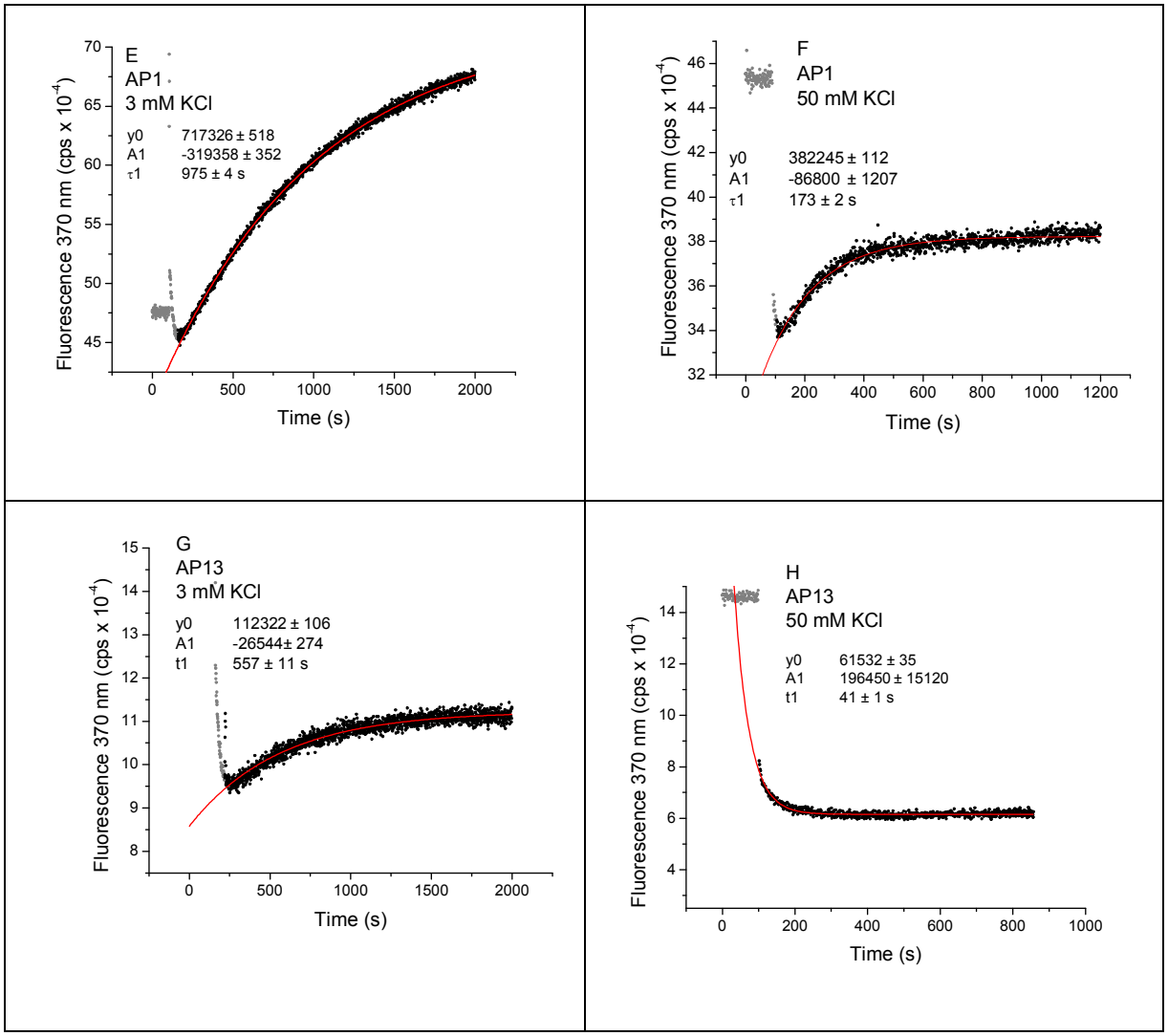

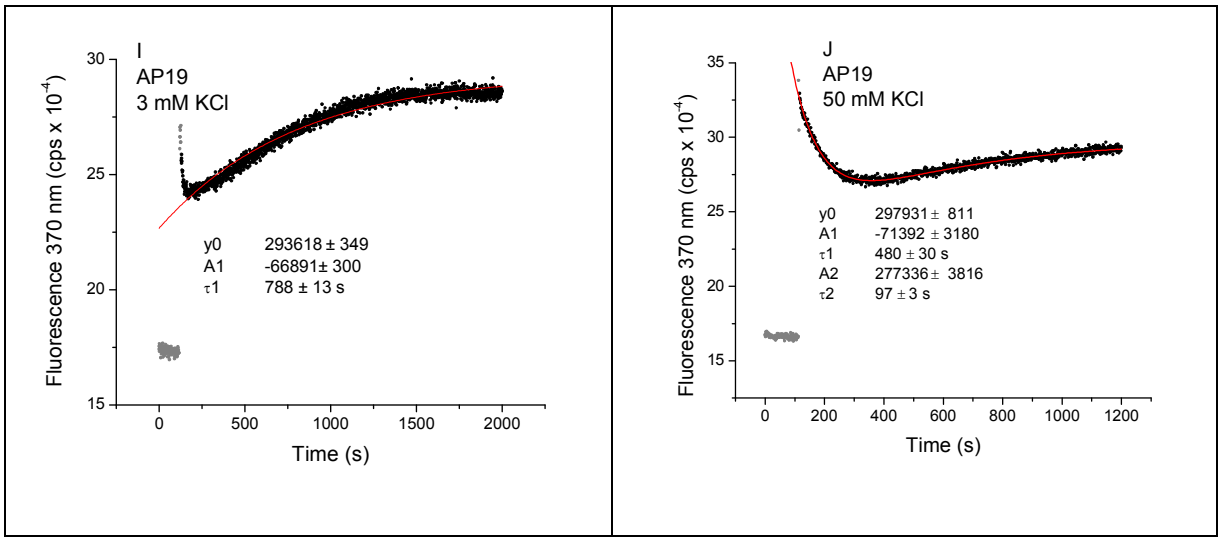
I
AP19
3 mM KCl
y0 293618 ± 349
A1 -66891± 300
τ1 788 ± 13 s
Fluorescence 370 nm (cps x 10^-4)
Time (s)
J
AP19
50 mM KCl
y0 297931± 811
A1 -71392 ± 3180
τ1 480 ± 30 s
A2 277336± 3816
τ2 97 ± 3 s
Fluorescence 370 nm (cps x 10^-4)
Time (s)

Figure S9. Na^+/K^+ exchange kinetics for 2-AP derivatives of Tel22. The exchange reaction was initiated by adding KCl from a 3M stock solution to a rapidly stirred solution of the indicated 2-AP derivative pre-equilibrated with 75 mM NaCl. The black traces show the change in fluorescence on adding KCl to a final concentration of 50 mM. The horizontal arrow indicates the starting value of the fluorescence in NaCl prior to addition of KCl. The vertical arrows indicate the rapid ("burst") fluorescence change that occurred during the ~5 s mixing time. The red line shows the best fit of the experimental data to single relaxation. *y0* is the final equilibrium value of the fluorescence, A_1 is the pre-exponential factor and τ_1 is the relaxation time. The errors are the standard deviation of the fitted parameters.

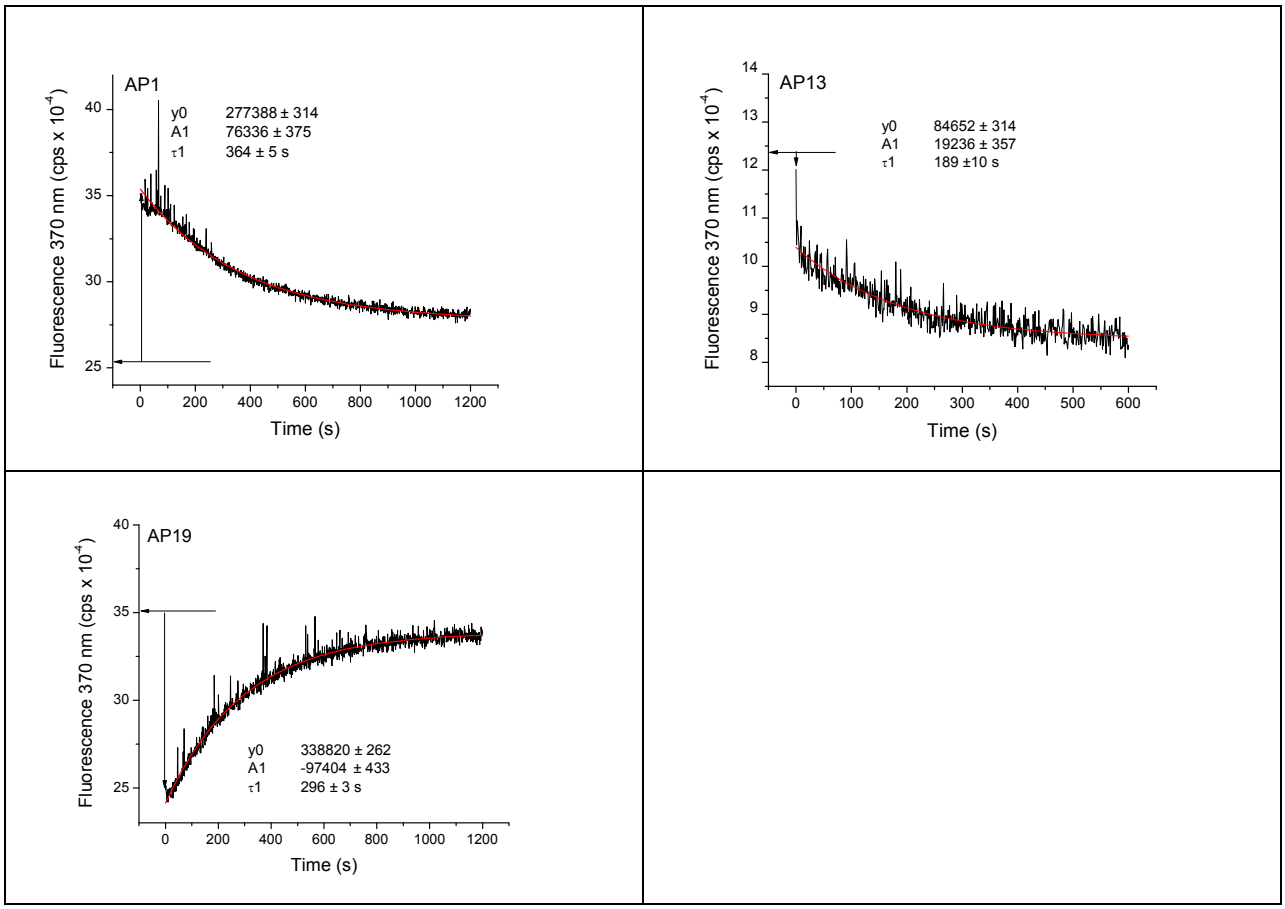

Figure S10. Simulated reaction profiles for linear and branched folding pathways as monitored by changes in fluorescence emission at a single wavelength. Fluorescence and concentration profiles were generated in SpecFit/32 for the specified mechanism. The relative fluorescence signal for each species is given in arbitrary fluorescence units (afu). The rate constants for each step in the sequence are shown in the figure. In both panels, the magenta curve represents the sum of the fluorescence of each species over the time course of the reaction. Note that only the sequential pathway shows a biphasic net change in emission over the time course of the reaction (magenta curves).

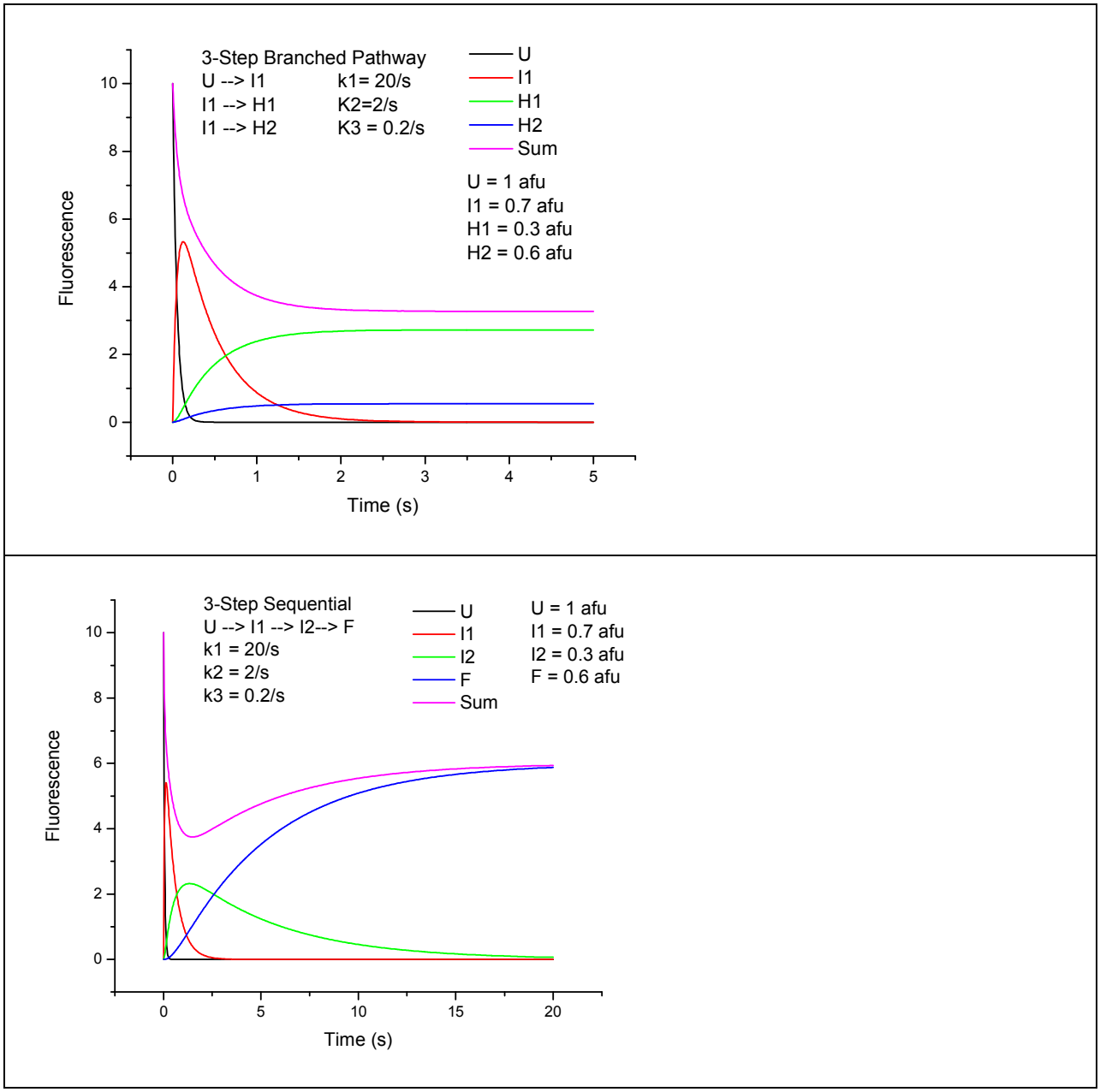

Table S1. NaCl, KCl concentrations and corresponding CD signals for titrations of Tel22 in Figures 4 and S2.

Figure S2		Figure 4	
[NaCl] (mM)	θ (millidegrees)	[KCl] (mM)	θ (millidegrees)
0	0.004	0	-0.083
0.05	0.086	0.025	0.594
0.10	0.114	0.049	1.496
0.15	0.084	0.074	2.617
0.25	0.148	0.099	3.946
0.35	0.576	0.123	5.262
0.44	0.340	0.148	6.474
0.64	0.466	0.173	7.662
0.84	0.722	0.197	8.824
1.03	1.133	0.247	10.330
1.23	1.378	0.296	11.692
1.42	2.062	0.394	13.619
1.72	2.630	0.492	15.523
2.11	4.913	0.589	16.696
2.50	6.667	0.785	17.978
2.89	8.802	0.979	19.020
3.47	11.041	1.174	19.634
4.25	13.357	1.477	20.206
5.02	13.357	1.780	20.581
5.61	14.448	2.385	20.818
6.57	15.171	2.988	20.914
8.02	15.944	4.996	21.015
9.95	16.400	7.000	21.163
12.84	16.729	12.999	21.061
18.61	17.066	24.951	20.989
24.36	16.948	48.664	21.137
36.31	17.355	95.353	21.411
60.01	17.311		
106.68	17.467		

REFERENCE

1. Gray, R. D., and Chaires, J. B. (2008) Kinetics and mechanism of K^+- and Na^+-induced folding of models of human telomeric DNA into G-quadruplex structures, *Nucleic Acids Res. 36*, 4191-4203.